Journal of Research in Science and Engineering (JRSE)
ISSN: 1656-1996 Volume-7, Issue-4, April 2025
DOI: 10.53469/jrse.2025.07(04).04

Dynamic Modeling and Analysis of a Mechanical Seal System Considering Shaft Stiffness

Mingtao Liu, Jiahao Li*, Gang Chen

College of Mechanical Engineering, Tianjin University of Science &Technology, Tianjin 300222, China
**Correspondence Author*

Abstract: ***In the petrochemical industry, mechanical seal systems used in centrifugal pumps often operate under medium-speed and light-load conditions. Component vibrations can cause dynamic variations in opening force and slight displacements, leading to failures such as seal face wear and leakage. This study considers the influence of shaft elasticity and introduces oil film stiffness parameters to establish a refined dynamic model of a coupled mechanical seal system comprising the rotating ring, stationary ring, and spindle. The model is used to analyze the variation patterns of axial displacement, radial displacement, and opening force of the components under different rotational speeds. The results show that the fluctuation frequency of the opening force is positively correlated with the rotational speed. An increase in speed intensifies the vibrational frequency of the axial displacement of the rotating ring, resulting in reduced stability. The axial displacement of the stationary ring exhibits good temporal dynamic stability. When the rotational speed reaches 1200 r/min, the vibration frequency of the shaft's radial displacement approaches the natural frequency of the shaft system, leading to seal face wear and failure.***

Keywords: Centrifugal pump mechanical seal system, Refined dynamic modeling, Oil film stiffness, Dynamic characteristics**.**

1. Introduction

Centrifugal pump mechanical seal systems are widely used in the petrochemical industry, where their sealing performance directly impacts on-site operations and personnel safety. Mechanical seals play a critical role in ensuring the normal operation of centrifugal pumps by preventing liquid leakage, stabilizing internal pressure, and blocking the ingress of air and contaminants. However, under real working conditions, seal components are prone to vibrations, which may cause lubrication film failure, dry friction at the sealing interfaces, reduced sealing performance, and even fatigue failure of the seal components. Therefore, it is of great significance to analyze the influencing factors of sealing performance, construct refined dynamic models, and investigate the dynamic characteristics of the system.

This study focuses on a contact-type mechanical seal system, in which sealing is achieved through close contact between the rotating ring and the stationary ring, forming a narrow sealing gap. In the field of contact-type mechanical seals, both domestic and international scholars have made substantial contributions. Hui Yuxiang studied oil-lubricated narrow-end-face contact seals [1], assuming uniform radial wear on the end face and obtained leakage and other performance parameters. Wei Long investigated the influence of operational parameters and fractal characteristics of surface morphology on the friction coefficient of seal faces through theoretical simulation and experimentation [2–4]. Bi Haocheng explored the friction mechanism under mixed lubrication conditions and analyzed the effect of operating conditions on sealing friction parameters [5]. Ding Xuexing developed a model for predicting average film thickness and analyzed trends in leakage rate and average film thickness under given working conditions [6–7]. Xingya Ni proposed a theoretical model for leakage rate of contact mechanical seals based on porous media fractal theory [8], providing a novel method for calculating seal leakage.

As a medium-speed rotating structure, the mechanical seal system of a centrifugal pump exhibits coupled bending and torsional vibrations among the rotating ring, stationary ring, and spindle, resulting in complex nonlinear dynamic behaviors. Investigating the dynamic responses of opening force and sealing performance under such conditions is crucial. Li Cunsheng developed a bending-torsion coupling vibration model for multi-disk rotors under seal fluid excitation and found that the system exhibits quasi-periodic motion with potential instability [9]. Zou Xinheng reported that low-frequency resonance in mechanical seals leads to severe wear at the outer diameter of the rotating ring [10]. Zhao Ziheng built a fluid-solid coupling model of a high-speed hydrostatic-hydrodynamic sliding bearing system to analyze the influence of bearing deformation on oil film characteristics [11]. Jin Saisai constructed a seal vibration system and investigated the system's responses under different excitations [12]. Wu Hao proposed the concept of comprehensive stiffness and developed an analytical model for calculating the comprehensive stiffness of rolling bearings [13]. Brenne conducted experimental studies on hydraulic excitation forces in centrifugal pump impellers [14]. Patir introduced the average flow model [15]. David B. Stefanko adopted several technical strategies—including controlling operating speed, redesigning bearings, and adjusting pump stiffness—to reduce radial vibrations and extend mechanical seal life [19].

Most of the above studies have focused on analyzing factors influencing leakage, vibration characteristics, and vibration suppression methods in contact-type mechanical seals. However, there is a lack of refined dynamic modeling for mechanical seal systems. For centrifugal pump mechanical seals used in the petrochemical industry, it is essential to explore the effects of seal face wear and deformation on sealing performance. Specifically, understanding how oil film stiffness, torsional stiffness of the rotating ring, and bending stiffness of the spindle affect the dynamic characteristics of the sealing system is critical.

In this study, a centrifugal pump mechanical seal system is selected as the research object. A refined dynamic model considering spindle elasticity is established based on Newtonian mechanics. In modeling the oil film stiffness, fluid-solid coupling finite element analysis is employed to obtain pressure distributions of the oil film between the rotating ring, stationary ring, and spindle. The bending stiffness of the spindle is calculated using the superposition method. The dynamic responses of axial displacement, radial displacement, and opening force under various rotational speeds are analyzed to characterize how rotational speed influences the sealing performance of the centrifugal pump mechanical seal system.

2. Structure and Working Principle of the Mechanical Seal System

The core components of a mechanical seal are the rotating ring, stationary ring, and drive shaft. The end faces of the rotating and stationary rings are tightly fitted to form a complete sealing ring, thereby enabling effective control of the rotating shaft. An axial compensation mechanism, such as a spring or bellows, is installed on one side of the rotating ring, serving as the compensation ring. The structural diagram of the centrifugal pump mechanical seal system is shown in Figure 1.During operation, the rotating ring1 rotates along with the shaft 3 and is simultaneously pressed against the stationary ring 2 by the compensation force provided by the compensation mechanism 5, ensuring close contact between the two rings. The stationary ring 2 is fixed to the stationary ring seat 7, which is secured to the pump casing.

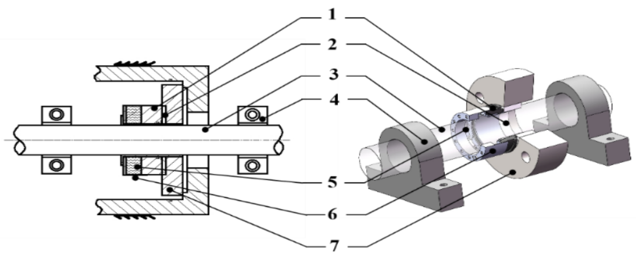

1- Rotating Ring, 2- Stationary Ring, 3- Shaft, 4- Support Base, 5- Spring, 6- Rotating Ring Seat, 7- Stationary Ring Seat

Figure 1: Schematic Diagram and 3D Model of the Centrifugal Pump Mechanical Seal System

In the centrifugal pump mechanical seal system, the high-speed rotation of the shaft 3 drives the rotating ring 1 to rotate. Relying on the compensating force provided by the elastic element 5 and the pressure of the sealing medium, an appropriate pressing force is generated at the contact interface between the rotating ring 1 and the stationary ring 2. This ensures close contact between the sealing faces and simultaneously forms a micron-scale lubricating film, thereby achieving an effective sealing function.

3. Refined Dynamic Modeling of the Mechanical Seal System

During the operation of a centrifugal pump mechanical seal system, the shaft is driven by an input torque, which in turn causes torsional deformation of the rotating ring. This torsional deformation can affect the sealing performance of the system. To maintain generality while avoiding excessive mathematical complexity, the following simplifications and assumptions are made in the development of the dynamic model for the mechanical seal system:

(1) rotating ring rotates at the same speed as the shaft.

(2) forces exerted by the fluid in the sealing chamber on both the rotating ring and the shaft are uniformly distributed.

3.1 Lumped Parameters and Generalized Coordinates

In the centrifugal pump mechanical seal system, the key components that affect sealing performance include the rotating ring, rotating ring seat, compensation mechanism, stationary ring, stationary ring seat, and the shaft. To simplify the model, the stationary ring, rotating ring, and shaft are treated as lumped mass elements, denoted as m1, m2, and m3, respectively, resulting in a total of three lumped parameters.

To accurately reflect the dynamic characteristics of the mechanical seal system while ensuring model precision, the following considerations are made: the shaft is subjected to an input torque that drives the rotation of the rotating ring; the stationary ring is mounted within the stationary ring seat. The model accounts for small displacements in the x, y, and z-directions among the rotating ring, stationary ring, and shaft, as well as torsional motion of the rotating ring and shaft about the x-axis.

Therefore, the generalized coordinates include three translational degrees of freedom for the stationary ring, three translational degrees of freedom for both the rotating ring and the shaft, and one rotational degree of freedom around the x-axis for the rotating ring-shaft assembly, resulting in a total of 11 generalized coordinates. The generalized coordinate vector is expressed as:

$$q = (x_1, y_1, z_1, x_2, y_2, z_2, \theta_1, x_3, y_3, z_3, \theta_2)^T \tag{1}$$

In the modeling process, the influence of shaft elasticity is considered, and the lumped parameter method is adopted to establish an 11-degree-of-freedom dynamic model of the mechanical seal system, as shown in Figure 2.

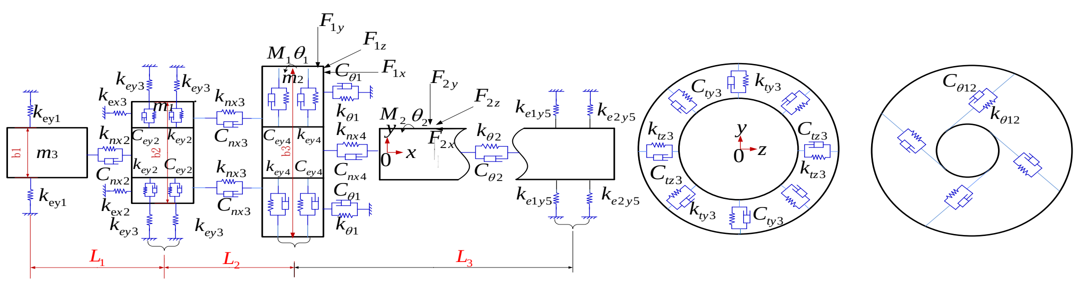

Figure 2: Dynamic Model of the Centrifugal Pump Mechanical Seal System

k_{ey1}, k_{e1y5}, k_{e2y5} is the contact stiffness between the main shaft and the bearing with its housing,

k_{ey2} is the contact stiffness between the stationary ring and the main shaft,

k_{ey4}, k_{nx4} is the contact stiffness between the rotating ring and the main shaft,

k_{ex3}, k_{ey3} is the contact stiffness between the stationary ring and its housing,

k_{nx3}, k_{ty3}, k_{tz3} is the contact stiffness between the rotating ring and the stationary ring,

$k_{\theta 1}$ is the torsional stiffness of the rotating ring,

$k_{\theta 2}$ is the torsional stiffness of the main shaft,

$k_{\theta 12}$ is the relative torsional stiffness between the rotating ring and the main shaft.

3.2 Dynamic Equation

Considering the contact stiffness between the rotating ring and the stationary ring, the rotating ring and the shaft, and the stationary ring and the shaft, as well as the torsional stiffness of the rotating ring and the shaft, along with the torsional moments and excitation forces acting on both the rotating ring and the shaft, the system's differential equations of motion are established based on Newton's second law. The dynamic equations of the stationary ring, rotating ring, and shaft in the mechanical seal assembly are as follows.

Stationary Ring: Translational Equation of Motion

$$\begin{cases} m_1\ddot{x}_1 + (k_{nx3} + k_{nx4})x_1 - k_{nx3}x_2 - k_{nx4}x_3 = 0 \\ m_1\ddot{y}_1 + \left(k_{ey3} + k_{ty3}\right)y_1 - k_{ty3}y_2 - k_{ey2}y_3 = 0 \\ m_1\ddot{z}_1 + (k_{ez3} + k_{tz3})z_1 - k_{tz3}z_2 - k_{ez2}z_3 = 0 \end{cases} \quad (2)$$

Rotating Ring: Translational Equation of Motion

$$\begin{cases} m_2\ddot{x}_2 - k_{nx3}x_1 + (k_{nx4} + k_{nx3})x_2 - k_{nx4}x_3 = F_{1x} \\ m_2\ddot{y}_2 - k_{ty3}y_1 + \left(k_{ey4} + k_{ty3}\right)y_2 - k_{ey4}y_3 = F_{1y} \\ m_2\ddot{z}_2 - k_{tz3}z_1 + (k_{tz3} + k_{ez4})z_2 - k_{ez4}z_3 = F_{1z} \end{cases} \quad (3)$$

Rotational Equation of Motion

$$m_2L_2^2\ddot{\theta}_1 - k_{\theta 1}L_1L_2\theta_1 + (k_{\theta 1} + k_{\theta 12})L_2^2\theta_1 - k_{\theta 12}L_2L_3\theta_2 = M_1 \quad (4)$$

Shaft: Translational Equation of Motion

$$\begin{cases} m_3\ddot{x}_3 - k_{nx4}(x_1 + x_2) + (k_{nx4} + k_{nx2})x_3 = F_{2x} \\ m_3\ddot{y}_3 - k_{ey4}(y_1 + y_2) + \left(k_{ey4} + k_{ey2}\right)y_3 = F_{2y} \\ m_3\ddot{z}_3 - k_{ez4}(z_1 + z_2) + (k_{ez2} + k_{ez4})z_3 = F_{2z} \end{cases} \quad (5)$$

Rotational Equation of Motion

$$m_3L_2^2\ddot{\theta}_2 - k_{\theta 12}L_3L_2\theta_1 + [k_{\theta 12}L_3 + k_{\theta 2}(L_1 + L_2)]\theta_2 = M_2 \quad (6)$$

F_{1x} is the x-direction component of the fluid excitation force acting on the rotating ring,

F_{1y}, F_{1z} are the y- and z-direction components of the fluid excitation force acting on the rotating ring,

F_{2x} is the x-direction excitation force on the shaft generated by engine rotation,

F_{2y}, F_{2z} are the y- and z-direction excitation forces on the shaft generated by engine rotation,

M_1 is the torsional moment acting on the rotating ring,

M_2 is the torsional moment acting on the shaft,

θ_1 is the torsional angle of the rotating ring,

θ_2 is the torsional angle of the shaft.

3.3 Bending Stiffness Calculation

Using the superposition method, the force exerted by the stationary ring on the shaft is simplified as F_1, and the force exerted by the rotating ring on the shaft is simplified as F_2. Based on this, an equivalent bending stiffness model for the shaft in the y-direction is established, as shown in Figure 3.

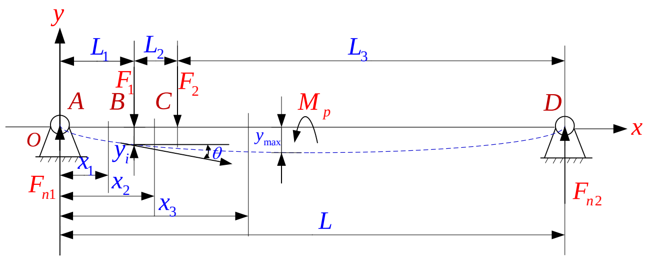

Figure 3: Mechanical Seal System Bending Stiffness Model

According to the principle of superposition for small displacements, the deflections at simply supported points B and C can be expressed as the linear superposition of individual deflections. Therefore, the deflections at points B and C are given by:

$$\begin{aligned} \omega_B &= \omega_{B1} + \omega_{B2} \\ &= -\frac{L_1(L_2+L_3)[L^2-L_1^2-(L_2+L_3)^2]}{6EIL}F_1 - \frac{L_1L_3\left(L^2-L_1^2-L_3^2\right)}{6EIL}F_2 \end{aligned}$$

$$\begin{aligned} \omega_C &= \omega_{C1} + \omega_{C2} \\ &= -\frac{(L_2+L_3)}{6EIL}\left\{\frac{L}{L_2+L_3}L_2^3 + [L^2 - (L_2 + L_3)^2](L_1 + L_2) - (L_1 + L_2)^3\right\}F_1 - \frac{L_3(L_1+L_2)[L^2-L_3^2-(L_1+L_2)^2]}{6EIL}F_2 \end{aligned} \quad (7)$$

After substituting the expressions of the flexibility coefficients with appropriate variables and incorporating the positional parameters x corresponding to various concentrated masses, the resulting system equations can be reformulated in matrix form. Accordingly, the lateral stiffness matrix k of the shaft system is given by:

$$k = \begin{bmatrix} \delta_{11} & \delta_{12} \\ \delta_{21} & \delta_{22} \end{bmatrix}^{-1} \quad (8)$$

3.4 Bending Stiffness Calculation

During the rotation of the centrifugal pump mechanical seal, a micron-scale oil film forms between the rotating ring and the stationary ring. The oil film thickness is calculated using the Hamrock–Dowson [16-17] film thickness formula (9):

$$h = 1.4\left(\frac{U}{W}\right)^{0.45}\left(\frac{E}{H}\right)^{0.55}\left(\frac{L}{R}\right)^{0.7} \tag{9}$$

The oil film thickness between the rotating and stationary rings is calculated as followsh_0=3.43μm.

Oil Film Stiffness:

$$k_e = \lim_{\substack{VF_r \to 0 \\ Vh \to 0}} \frac{VF_r}{Vh'} = \left(\frac{dh'}{dF_r}\right)^{-1} \tag{10}$$

Based on the Hertz contact model for elastic bodies in contact, the contact stiffness KHK_HKH between the rotating and stationary rings is given by:

$$k_c = \left(\frac{d\delta}{dF_r}\right)^{-1} \tag{11}$$

Comprehensive contact stiffness between the rotating ring and the stationary ring can be expressed as:

$$k_{nx3} = \left(\frac{1}{k_e} + \frac{1}{k_c}\right)^{-1} \tag{12}$$

4. Numerical Example

4.1 Bending Stiffness Calculation

Table 1 presents the main structural dimensions of the core components of the centrifugal pump mechanical seal, namely the shaft, the rotating ring, and the stationary ring.

Table 1: Structural Dimension Parameters of Mechanical Seal System Components

Structural Parameter	Shaft	Rotating Ring	Stationary Ring
Outer Diameter (mm)	57	80	75
Inner Diameter (mm)	-	63	60
Length (m)	1.5	0.03	0.01
Center Distance (m)	L_1=0.2 L_2=0.15 L_3=1.15		

The excitation force and torque experienced by the dynamic ring and shaft of the centrifugal pump mechanical seal are shown in Table 2.

Table 2: Dynamic Ring and Shaft Force and Moment Parameters

Force Parameters	Dynamic Ring	Shaft
Excitation Force	$F_1 = 189.3N$	$F_2 = 191.6N$
Input Torque	$M_1 = 64.43N \cdot m$	$M_2 = 79.57N \cdot m$
Torsion Angle	$\theta = 0.00856°$	$\theta = 0.03303°$

4.2 Stiffness Parameters

1) Bending Stiffness Calculation

By solving equation (7), the variation pattern of the flexibility coefficient throughout the shaft system is obtained, as shown in Figure 4.

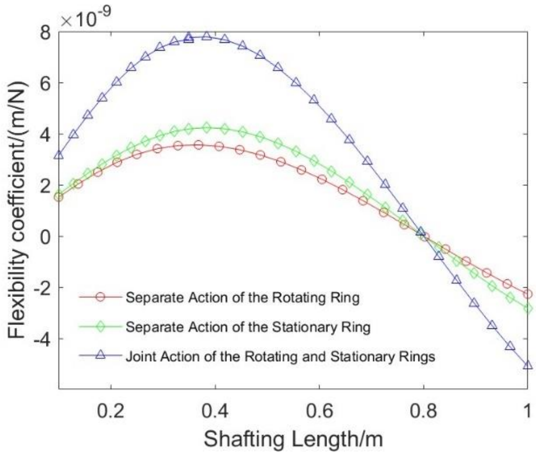

Figure 4: Shaft Flexibility Coefficient

Unit forces is applied to the positions of the dynamic ring and static ring, and the deformation amounts at the positions of the two particles are inverted to obtain the stiffness matrix of the shaft system.

$$K = \begin{bmatrix} -6.1078e^9 & 5.1937^9 \\ 5.1937^9 & -4.6551e^9 \end{bmatrix}$$

2) Oil Film Stiffness Calculation.

Simulation analysis of the oil film pressure between the dynamic ring and static ring is conducted in the ANSYS environment, and the oil film pressure contour map is shown in Figure 5.

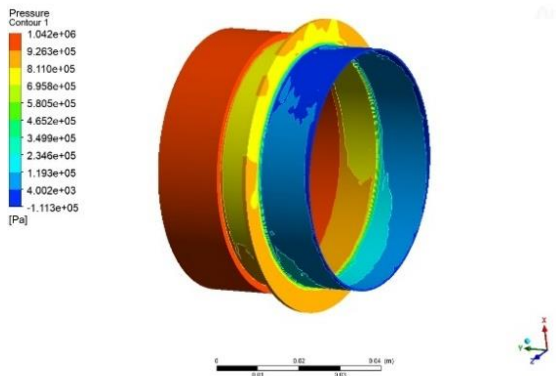

Figure 5: Oil Film Pressure Contour Map

Based on equations (9) to (12), the oil film stiffness, Hertzian contact stiffness, and comprehensive contact stiffness at the contact end faces of the dynamic and static rings in the mechanical seal system are calculated. The stiffness parameters are shown in Table 3.

Table 3: Stiffness Parameters of the Contact End Faces Between Dynamic and Static Rings

Stiffness Parameter	Value
Oil Film Stiffness	$k_e = 6.66 \times 10^5 \mathrm{N/m}$
Herz Contact Stiffness	$k_c = 4.32 \times 10^8 \mathrm{N/m}$
Comprehensive Contact Stiffness	$k_{nx3} = 6.66 \times 10^5 \mathrm{N/m}$

The calculation results indicate that the oil film stiffness parameter directly influences the contact stiffness at the interface between the dynamic and static rings. Under actual operating conditions, when the oil film stiffness increases within a certain range and the film thickness remains relatively stable, the stability of the sealing system can be improved, and frictional power loss can be reduced. However, when the oil film stiffness deviates from its optimal value, frictional power loss increases significantly, leading to excessive wear on the sealing surfaces, which negatively affects sealing performance and the normal operation of the equipment. Therefore, calculating the oil film stiffness parameter is essential for evaluating the stability of the sealing system.

The torsional stiffness of the dynamic ring refers to its ability to resist torsional deformation. It is typically quantified by the torsional stiffness coefficient, which is numerically equal to the torque required to produce a unit torsional angle in the dynamic ring.

The length of the dynamic ring is $L_1 = 0.03m$, and the elastic modulus is $G = 5GPa$.

The torsional angle of the dynamic ring can be obtained through calculation.

$$\theta_1 = 2.1 \times 10^{-7}\text{rad}$$

Dynamic Ring Torsional Stiffness,

$$k_{\theta 1} = \frac{T}{\theta_1} = 6.67 \times 10^8 \text{Nm/rad}$$

The dynamic parameters of the shaft, dynamic ring and its seat, and the static ring and its seat in the centrifugal pump mechanical seal assembly are shown in Table 4.

Table 4: Dynamic Parameters of the Mechanical Seal System

Parameter	Shaft	Dynamic Ring and Dynamic Ring Seat	Static Ring and Static Ring Seal
Mass (kg)	4.34	2.4	7.92
Moment of Inertia (kg·m2)	0.0141	0.0154	0.2566
Torsional Stiffness (Nm/rad)	$k_{\theta 1} = 6.67e^8$ $k_{\theta 2} = 1.08e^8$ $k_{\theta 12} = 4.47e^8$		
Contact Stiffness (N/m)	$k_{ex2} = 8.8e^6$ $k_{ex3} = 9.2e^6$ $k_{ey2} = k_{ez2} = 5.8e^8$ $k_{ey3} = k_{ez3} = 6.8e^8$ $k_{ey4} = k_{ez4} = 6.4e^8$ $k_{nx2} = 5.6e^6$ $k_{nx3} = 6.6e^5$ $k_{nx4} = 2.63e^7$ $k_{ty3} = k_{tz3} = 4.6e^7$		

4.3 Stiffness Parameters

4.3.1 Time-domain analysis of activating force

In the mechanical seal device of a centrifugal pump, studying the dynamic characteristics of the activating force at different rotational speeds can reflect the variation law of the sealing performance. For three different rotational speeds of 800 r/min, 1200 r/min, and 1600 r/min, the dynamic equations (2)–(7) are used, with the stiffness parameters substituted. The response time is set to 5 seconds, and the theoretical solution for the time history of the activating force between the contact end faces of the dynamic and static rings is obtained, as shown in Figure 6.

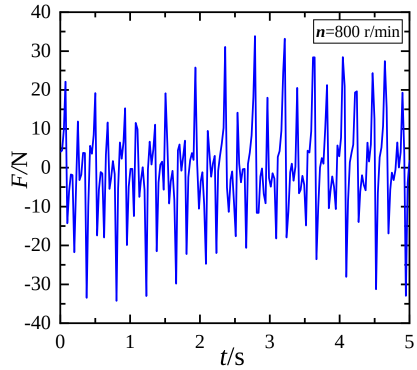

(a) n=800 r/min

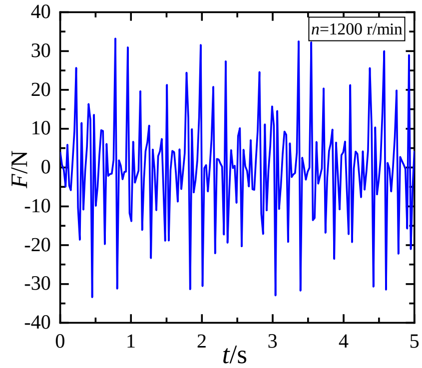

(b) n=1200 r/min

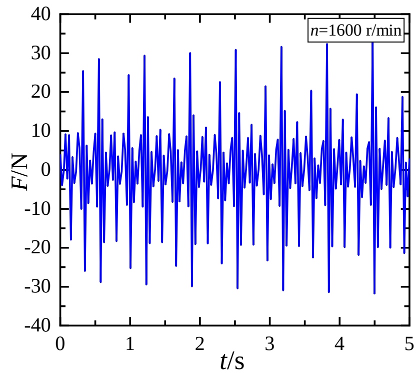

(c) n=1600 r/min

Figure 6: Time history of activating force at different rotational speeds

From Figure 6, it can be observed that under the influence of the input torque, the activating force vibration amplitude at 1600 r/min is significantly larger than that at 1200 r/min and 800 r/min. The vibration amplitudes are 30 N, 25 N, and 20 N, respectively. Comparing the results in Figures (a), (b), and (c), it is found that the fluctuation amplitude and frequency of the activating force increase with the rotational speed. This indicates that, under working conditions, as the rotational speed increases, the vibration frequency of the activating force rises, forcing more frequent relative motion between the dynamic and static rings. This accelerates the wear of the sealing end faces and reduces the sealing performance of the mechanical seal system.

4.3.2 Time-Domain Analysis of Axial Displacement

To analyze the influence of small displacements on sealing performance under different rotational speed conditions, a dynamic response analysis of the axial displacement of the dynamic and static rings is carried out. The time-domain variation curves of the displacement of each component in the centrifugal pump mechanical seal device under different rotational speeds are obtained. The time-domain dynamic response curves of the axial displacement of the dynamic ring at 800 r/min, 1200 r/min, and 1600 r/min are shown in Figure 7.

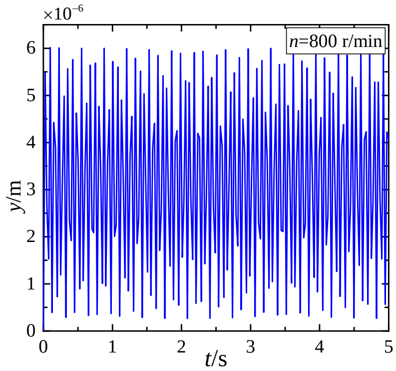

(a) *n*=800 r/min

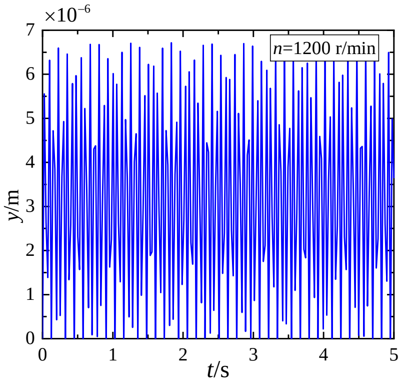

(b) *n*=1200 r/min

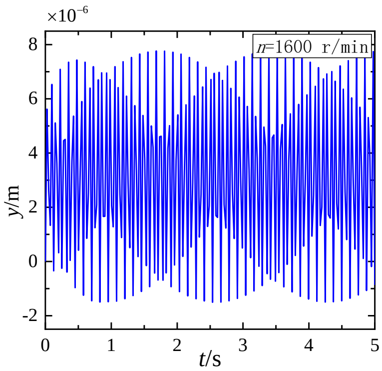

(c) *n*=1600 r/min

Figure 7: Time history of axial displacement of the dynamic ring at different rotational speeds

From Figure 7, it can be seen that under the influence of transmitted torque, the axial displacement response of the dynamic ring at 1600 r/min is significantly greater than that at 1200 r/min and 800 r/min. The maximum axial displacement responses of the dynamic ring at 800 r/min, 1200 r/min, and 1600 r/min are 6 µm, 6.5 µm, and 7 µm, respectively. Comparing the results in Figures (a), (b), and (c), it is found that the axial displacement response of the dynamic ring is positively correlated with the rotational speed. This indicates that an increase in speed leads to larger axial displacement of the dynamic ring, which raises local pressure on the sealing end face, accelerates wear, and results in noticeable scratches and wear grooves on the sealing surface, thereby reducing sealing performance. Therefore, in practical applications, increasing the width of the sealing face, reducing the specific pressure on the sealing surface, or selecting a suitable spring stiffness can help reduce the axial displacement of the dynamic ring and mitigate wear on the sealing surface.

The time-domain dynamic response curves of the axial displacement of the static ring at rotational speeds of 800 r/min, 1200 r/min, and 1600 r/min are shown in Figure 8.

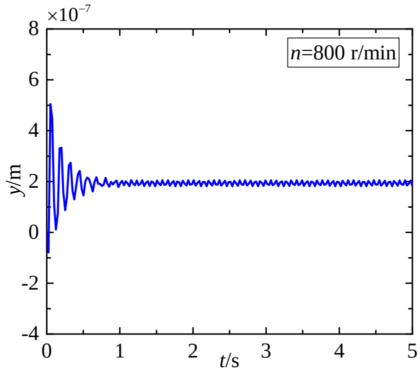

(a) *n*=800 r/min

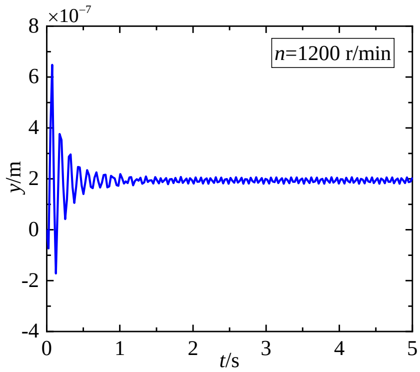

(b) *n*=1200 r/min

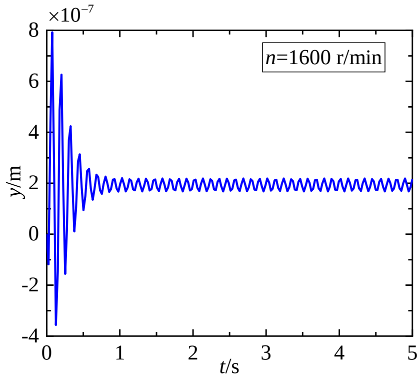

(c) *n*=1600 r/min

Figure 8: Time history of axial displacement of the static ring at different rotational speeds

From Figure 8, it can be seen that under the action of friction between the dynamic and static rings, the axial displacement response of the static ring at 1600 r/min is greater than that at 1200 r/min and 800 r/min. The maximum axial displacement responses of the static ring at 800 r/min, 1200 r/min, and 1600 r/min are 0.5 µm, 0.65 µm, and 0.8 µm, respectively. Comparing the results in Figures (a), (b), and (c), it is found that although the axial displacement of the static ring is significantly affected by rotational speed during the startup phase, its steady-state amplitude remains within a relatively small and stable range, fluctuating around 0.2 μm [18]. This indicates that during the startup process of the centrifugal pump mechanical seal device, the static ring's axial displacement is more susceptible to low-frequency vibrations, but the displacement values are far smaller than the contact clearance between the dynamic and static rings, ensuring good sealing performance at the contact end faces.

4.3.3 Time-Domain Analysis of Radial Displacement

To analyze the influence of small displacements on sealing performance under different rotational speed conditions, a dynamic response analysis of the radial displacement of the shaft and the dynamic ring is carried out. The time-domain dynamic response curves of the shaft's radial displacement at the contact position of the dynamic and static ring end faces at rotational speeds of 800 r/min, 1200 r/min, and 1600 r/min are shown in Figure 9.

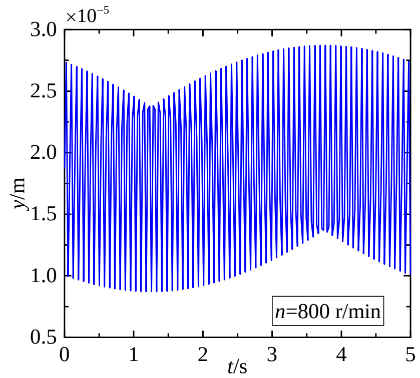

(a) n=800 r/min

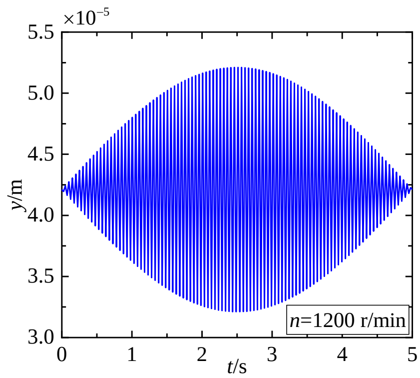

(b) n=1200 r/min

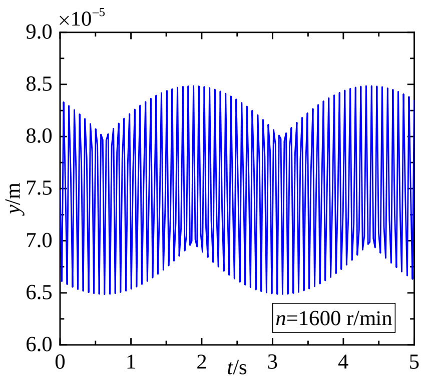

(c) n=1600 r/min

Figure 9: Time history of shaft radial displacement at the contact end face position of the dynamic and static rings under different rotational speeds.

From Figure 9, it can be seen that under the influence of the input torque, at the contact end face position of the dynamic and static rings, the radial displacement response of the shaft at 1600 r/min is significantly greater than that at 1200 r/min and 800 r/min. The maximum radial displacement responses of the shaft at 800 r/min, 1200 r/min, and 1600 r/min are 27.5 μm, 52.5 μm, and 83 μm, respectively. Comparing the results in Figures (a), (b), and (c), it is found that the vibration amplitude and frequency of the radial displacement increase significantly with the rotational speed. However, at a rotational speed of 1200 r/min, the vibration frequency approaches the natural frequency of the shaft system, causing the amplitude of the radial displacement to change regularly, which leads to overall machine vibration and may even reduce the sealing performance of the system.

The time-domain dynamic response curves of the radial displacement of the dynamic ring at the contact position of the dynamic and static ring end faces at rotational speeds of 800 r/min, 1200 r/min, and 1600 r/min are shown in Figure 10.

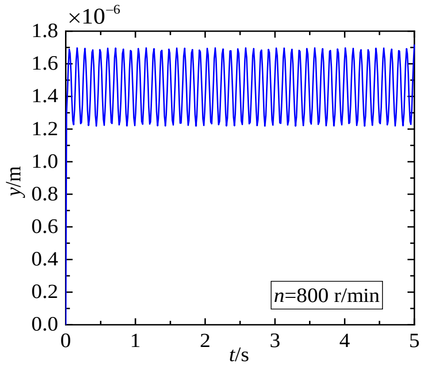

(a) n=800r/min

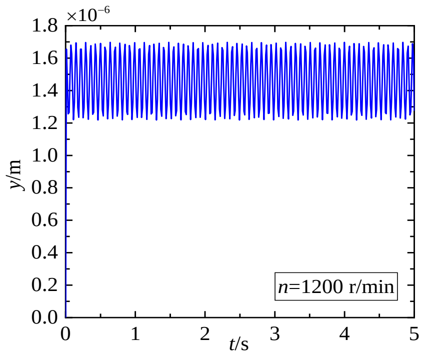

(b) n=1200r/min

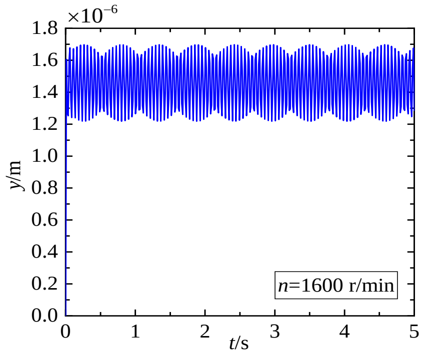

(c) n=1600r/min

Figure 10: Radial displacement time history of the moving ring at different rotational speeds.

As shown in Figure 10, under the influence of the transmitted torque, when the rotational speed of the moving ring increases gradually from 800 r/min to 1200 r/min, the radial displacement vibration amplitude of the moving ring remains relatively stable, fluctuating around the magnitude of 1.5 μm. However, the radial displacement vibration frequency of the moving ring increases significantly. Comparing the results in Figures (a), (b), and (c), it is observed that the increase in the radial displacement frequency of the moving ring leads to uneven changes in the sealing gap between the moving and stationary rings, which increases the leakage. This also alters the compression and force conditions of the spring, potentially causing spring fatigue failure. The vibration signal is transmitted to other components of the centrifugal pump, such as the impeller and shaft, resulting in increased overall machine vibration, affecting the normal operation of the equipment, and even leading to equipment failure.

4.3.4 Frequency Domain Analysis

The Fast Fourier Transform (FFT) converts the time-domain variation of the excitation force at different rotational speeds into frequency-domain variations, as shown in Figure 11.

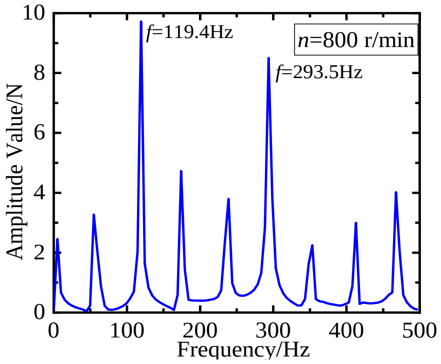

(a) *n*=800 r/min

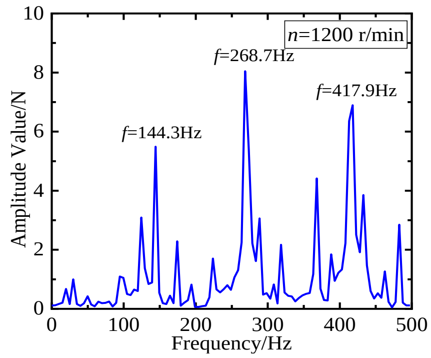

(b) *n*=1200 r/min

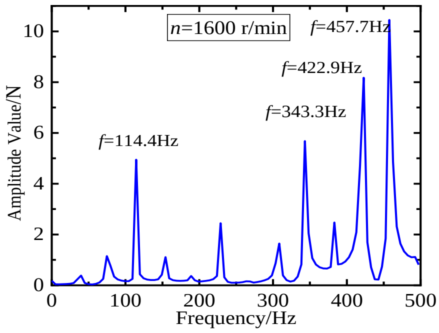

(c) *n*=1600 r/min

Figure 11: Frequency domain response of the sealing end face excitation force at different rotational speeds

As shown in Figure 11, the frequency domain response of the excitation force exhibits multiple peaks at different rotational speeds. In Figure (a), the main peak frequencies are 119.4 Hz and 293.5 Hz. In Figure (b), the main peak frequencies are 144.3 Hz, 268.7 Hz, and 417.9 Hz. In Figure (c), the main peak frequencies are 114.4 Hz, 343.3 Hz, 422.9 Hz, and 457.7 Hz. Comparing Figures (a), (b), and (c), it can be seen that an increase in rotational speed leads to a rise in the frequency peak values of the centrifugal pump, which improves the pump's efficiency but reduces its lifespan.

In Figure (b), the vibration amplitude of the excitation force remains relatively stable without any sudden peak values. Mechanical vibration and wear are relatively small, maintaining good operational stability and lifespan. This ensures that the centrifugal pump's mechanical seal leakage remains stable, reduces sealing surface wear, lowers system energy consumption, and improves pumping efficiency. Therefore, in practical conditions, an engine speed of 1200 r/min is preferred.

5. Conclusion

This paper establishes a refined dynamic model of the mechanical seal system to investigate the effects of spindle bending deformation, moving ring torsional deformation, and oil film stiffness on sealing performance. The dynamic response analysis of the moving ring, stationary ring, and spindle is conducted, and the conclusions are as follows:

1) Time Domain Analysis of Opening Force: The results of the time-domain analysis of the opening force show that at rotational speeds of 800 r/min, 1200 r/min, and 1600 r/min, the vibration amplitudes of the opening force are 20 N, 25 N, and 30 N, respectively. The fluctuation frequency of the opening force is positively correlated with the rotational speed. As the centrifugal pump speed increases, the centrifugal force of the impeller increases, leading to higher fluid pressure within the pump, which in turn increases the pressure on the sealing end face of the mechanical seal device, causing the opening force to increase correspondingly.

2) Dynamic Response of Axial and Radial Displacements: The analysis of the time-domain dynamic response of the axial and radial displacements of the moving and stationary rings shows that as the rotational speed increases from 800 r/min to 1600 r/min, the axial displacement amplitude of the moving ring increases from 6 μm to 7 μm. The local pressure on the sealing end face increases, accelerating wear and resulting in visible scratches and wear grooves on the sealing surface, which reduces sealing performance. The axial displacement of the stationary ring fluctuates around 0.2 μm, exhibiting good stability in its dynamic characteristics.

3) Frequency Domain Analysis of Opening Force Amplitude Variation: The results of the frequency domain analysis of the variation in the opening force amplitude show that as the rotational speed increases from 800 r/min to 1600 r/min, the vibration frequency increases from 293.5 Hz to 457.7 Hz. At 1200 r/min, the system maintains a certain pumping efficiency with no sudden peak values in amplitude. This ensures stable leakage of the centrifugal pump's mechanical seal device, reduces wear on the sealing end face, lowers

system energy consumption, and improves pumping efficiency.

References

[1] Hui, Y., Liu, Y., Wang, Y., et al. (2021). A contact face sealing model considering wear and experiment. Tribology Transactions, 41(03), 316-324.
[2] Wei, L., Zhang, P., Liu, Q., et al. (2016). Analysis and experiments on the friction coefficient of contact mechanical seal end faces. Tribology Transactions, 36(03), 354-361.
[3] Wei, L., Zhang, P., Fang, G. (2020). Fractal model for mixed friction heat calculation on mechanical seal end faces. Hydraulics and Pneumatics, (07), 112-117.
[4] Wei, L., Chang, X., Zhang, P. (2012). Research progress on leakage models of contact mechanical seal end faces. Fluid Machinery, 40(02), 36-40.
[5] Bi, H., Hao, M., Ren, B., et al. (2023). Study on the friction evolution law of contact mechanical seal under mixed lubrication. Tribology Transactions, 43(11), 1241-1253.
[6] Zhao, Y., Ding, X., Wang, S. (2022). Mechanical seal leakage rate and film thickness prediction based on fractal contact theory. Lubrication and Sealing, 47(08), 156-163.
[7] Zhang, W., Xue, J., Li, J., et al. (2019). Axial vibration stability analysis of rotor-bearing-dry gas seal systems. Lubrication and Sealing, 44(05), 9-16.
[8] Xingya Ni, Chenbo Ma, Jianjun Sun, et al. (2021). A leakage model of contact mechanical seals based on the fractal theory of porous medium. Coatings, 11(1), 20.
[9] Liu, Z., Li, C., Huang, Z., et al. (2007). Research on the bending-torsion coupling vibration and bifurcation characteristics of turbine pump rotors. Rocket Propulsion, (05), 11-17.
[10] Zou, X., Chen, Q., Gao, L. (2021). Study and experimental analysis of the dynamic characteristics of the moving ring structure in mechanical seals. Lubrication and Sealing, 46(01), 111-116.
[11] Zhao, Z., Tan, Y., Ma, L., et al. (2025). Study on the oil film characteristics of ultra-high-speed liquid sliding bearings considering fluid-structure interaction. Lubrication and Sealing, 1-8.
[12] Jin, S., Sun, J., Ma, C. (2025). Study on the axial vibration system of non-contact mechanical seals based on the Newmark-β method. Lubrication and Sealing, 1-9.
[13] Wu, H. (2011). Study on the dynamic characteristics of rolling bearings and rotor-bearing system dynamics model. East China University of Science and Technology.
[14] Brennen, C., Acosta, A., Caughey, T. (1980). A test program to measure fluid mechanical whirl excitation forces in centrifugal pumps. NASA Lewis Research Center Rotordynamics Instability Problems in High-Performance Turbomachinery.
[15] Patir, N., Cheng, H. S. (1979). Application of average flow model to lubrication between rough sliding surfaces. Journal of Lubrication Technology, 101(2), 220-229.
[16] Sarangi, M., Majumdar, B. C., Sekhar, A. S. (2005). On the dynamics of elastohydrodynamic mixed lubricated ball bearings. Proceedings of the Institution of Mechanical Engineers - Part J - Journal of Engineering Tribology, 219(6), 411-421.
[17] Creju, S., Bercea, L., Mitu, N. (1995). A dynamic analysis of tapered roller bearings under fully flooded conditions. Part 1: Theoretical formulation. Wear, 188(1-2), 1-10.
[18] Wang, Z. (2024). Performance and vibration characteristics of mechanical seals in marine pumps under variable operating conditions. Beijing University of Chemical Technology.
[19] Stefanko, D. B., Leishear, R. A. (2005). Relationship between vibrations and mechanical seal failures in centrifugal pumps. ASME 2005 International Mechanical Engineering Congress and Exposition.

Author Profile

Mingtao Liu (1974-), female, Associate Professor, Ph.D. Her research interests include mechanism theory and mechanical transmission. E-mail: liumingtao@tust.edu.cn